ELSEVIER

Biophysical Chemistry 104 (2003) 459–468

Biophysical Chemistry

www.elsevier.com/locate/bpc

NMR investigation of the alkaline-like conformational transition of horse heart cytochrome *c* in the presence of exogenous thiazole

Yong Yao, Wenxia Tang*

State Key Laboratory of Coordination Chemistry, Nanjing University, Nanjing 210093, PR China

Received 27 October 2002; received in revised form 23 January 2003; accepted 23 January 2003

Abstract

The conformational transition of horse heart cyt *c* in the presence of exogenous thiazole is investigated by NMR spectroscopy. Surprisingly, besides the native form and the ligand-bound form, another species (species A) exists at neutral pH. Titration of thiazole at alkaline condition indicates that this form has Lys as the axial ligands and in fact is one of alkaline cyt *c* conformers. At a high concentration of thiazole, species A has a dominant population at a pH of approximately 7. It is the first time that a pure alkaline conformer of cyt *c* is obtained at neutral pH. The observed NOEs show that species A maintains the overall protein fold although large structural rearrangements are expected in the distal pocket. Furthermore, the different effect of imidazole, pyridine and thiazole on the alkaline transformation of cyt *c* is discussed.

Keywords: Cytochrome *c*; NMR; Thiazole; Conformational transition; Alkaline isomerization

1. Introduction

Mitochondria cytochrome *c* is an important hemoprotein that functions as an electron carrier in the electron transport chain [1,2]. The pH-dependent conformational transition of ferricytochrome *c* has been known for many years [3–10]. Of these conformations, the native state prevails at neutral pH and is converted to the alkaline forms with pK_a values between 8.5 and 9.5 depending on the species. The knowledge of the alkaline transition of cyt *c* is of intense interest for several reasons. First, studies have provided evidence that the structural changes involved in the alkaline transition may be related to the electron-transfer process of cyt *c* in the complexes with its natural reaction partners [11,12]. For example, Raman spectroscopy indicates the binding of cyt *c* to cyt *c* oxidase induces dissociation of Met80 from the heme iron in cyt *c*, an event required for formation of the alkaline forms. Second, the understanding of how proteins efficiently fold from a disordered state to a unique and fully functional native state is always an attractive area. The alkaline conformers may be regarded as intermediate state during the unfolding of cyt *c* [13–21]. NMR studies of the unfolding of cyt *c* in urea and guanidine hydrochloride show that under mild denature conditions, cyt *c* undergoes alkaline-like

---

*Corresponding author. Tel.: +86-25-3595706; fax: +86-25-3314502.

E-mail address: wxtang@netra.nju.edu.cn (W. Tang).

0301-4622/03/$ - see front matter © 2003 Elsevier Science B.V. All rights reserved.
doi:10.1016/S0301-4622(03)00031-0

conformational transition and the hyperfine shifts of the identified unfolding equilibrium intermediates are quite similar to those of the alkaline conformers [19,20]. Finally, recent investigations find cyt *c* undergoes structural changes in mixed aqueous–non-aqueous media, resulting in formation of alkaline-like species [22]. This fact leads to the proposal that near the mitochondrial membrane, a low dielectric environment, cyt *c* may exist in alkaline-like forms.

Although spectroscopic studies indicate that Met80 is substituted by Lys 73 or Lys 79 (or Lys 72 in some cases) as the sixth axial ligand, unambiguous structural characterization of the alkaline conformers is still lacking [7,8]. There are two factors that prevent from obtaining NMR structures of the alkaline cyt *c*. One is that an alkaline solution condition is not suitable for NMR experiments because the backbone NHs exchange fast with the solvent. The other is the complex interconvertible conformations coexisting in the alkaline solution. It has been found that mutation of residues located nearby Met80 and some nitrogenous ligands, for example, pyridine and its derivatives, will decrease the pK_a of the alkaline transition to approximately 7 [6,7,23–25]. However, it is still unsuccessful to get a pure alkaline conformer at neutral pH for NMR study. In this paper, we find that thiazole is a unique ligand in that it selectively stabilizes one conformer of the alkaline forms and in the presence of thiazole, a homogeneous alkaline conformer can be obtained at neutral pH. With the isotopic label technology, our results make it now feasible to determine the alkaline form of cyt *c* by NMR spectroscopy.

2. Materials and methods

2.1. Sample preparation

Horse heart cyt *c* (type VI) was purchased from Sigma Chemical Co. and purified as previously described [26]. Thiazole was bought from ACROS ORGANICS and its purity was check before use by NMR spectroscopy. The ^{1}H NMR samples were prepared by dissolving the lyophilized protein in D_2O. Concentrated thiazole solution was added to the protein solution to control the thiazole concentration. The pH was adjusted by addition small volumes of DCl or NaOD (uncorrected for the isotope effect). The final NMR samples contained approximately 2–4 mM hh cyt *c*.

2.2. NMR spectroscopy

The NMR spectra were collected on a Bruker DRX 500 spectrometer. One-dimensional superWEFT and superWEFT-NOE were carried out using reported methodology to optimize the paramagnetical signals [27,28]. Two-dimensional DQF-COSY, TOCSY and NOESY spectra were collected following standard pulse sequences [29]. NOESY maps in D_2O solution were recorded on a spectral width of 50 ppm with a recycle time of 600 ms and a mixing time of 50 ms. To optimize the observation of connectivities in the diamagnetic region, NOESY maps in D_2O solutions were recorded on a smaller spectral width (16 ppm), with recycle time of 1.2 s and a mixing time of 100 ms. Analogously, DQF-COSY and TOCSY experiments were recorded over the spectral width of 16 ppm (recycle time of 1.2 s and spin lock times of 70 ms). The EXSY spectra were acquired using the NOESY pulse sequence on a spectral width of 50 ppm with a mixing time of 25 ms or 50 ms.

The ^{1}H-^{13}C HMQC spectra were carried out using natural abundance samples without decoupling during acquisition [30]. The Δ delay was adjusted to optimize sensitivity according to the line widths of heme methyl signals. The chemical shifts were calibrated in the proton frequency using water as internal reference and in the carbon frequency using dioxane at 66.6 ppm.

Data processing was performed using the standard Bruker software package XWINNMR on a Silicon Graphics workstation, the two-dimensional spectra were analyzed with the aid of the program XEASY [31].

3. Results and discussion

3.1. Detection of an alkaline isomer of cyt c in the presence of thiazole at neutral pH

Fig. 1 depicts the NMR spectra of the hyperfine regions of cyt *c* in the presence of 1 M thiazole at

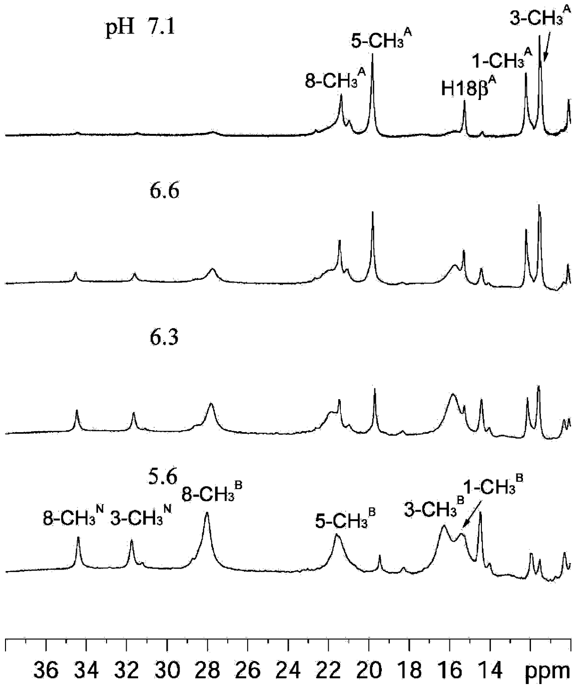

Fig. 1. The downfield hyperfine shifted region of cyt *c* spectra as a function of pH at 303 K in the presence of 1 M thiazole. Resonances due to native cyt *c*, thiazole-cyt *c* and species A are labeled with N, B and A, respectively.

pH ranging from 5.6 to 7.1. The chemical shifts of the four heme methyls of the thiazole–cyt *c* complex (labeled as B) could be easily identified in the EXSY spectrum (data not shown). To our surprise, another species (labeled as A) exists and increases at the expense of the native cyt *c* and the bound form as the pH increases. At pH 7.1, this species has a dominant population with well-resolved resonances. Since there are no cross-peaks between the native form and species A in the EXSY spectra at pH 7.1 and 303 K indicating species A undergoes very slow exchange of native cyt *c*, the hyperfine shifted resonances of this species are assigned based on HMQC and NOESY experiments (Fig. 2, see below).

As the chemical shifts of the four heme methyls and its hyperfine shift pattern of species A bear a strong similarity to the cyanide adducts of cyt *c* and the alkaline forms of cyt *c* (Table 1), it is speculated that the sixth axial ligands in species A

is of cylindric symmetry. Recently, Bowler et al. found that in yeast cyt *c*, the N-terminal amino group can ligate to the heme under denaturating conditions [20]. However, in cyt *c* of mammals such as horse heart cyt *c*, the N-terminal is acetylated [32], so the remaining candidate is a depro-

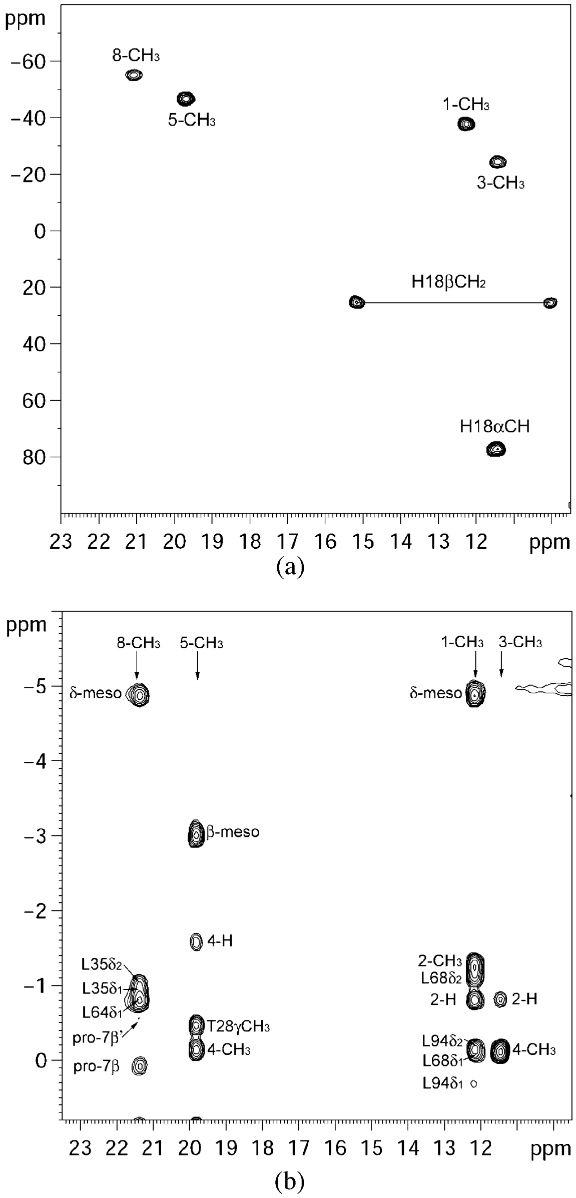

(a)

(b)

Fig. 2. Portions of HMQC (a) and NOESY (b) of species A at pH 7.1 and 303 K.

tonated Lys. It has been reported that the alkaline form of cyt *c* was a mixture of two Lys-ligated conformers and the ligated Lys is located at the loop encompassing residues 70–85 [1,4]. To verify the relationship between species A and the alkaline cyt *c* forms, a series of NMR experiments of cyt *c* at pH 9.5 and 303 K with varying concentration of thiazole were carried out (Fig. 3). From Fig. 3, it is seen that at such pH and temperature the NMR spectra show the presence of two alkaline forms (A_1 and A_2) which are in equilibrium with the native form and A_1 is highly populated as the concentration of thiazole is above 160 mM. It can be clearly noted that the spectrum of cyt *c* in the presence of 160 m thiazole at pH 9.5 is the same to that of cyt *c* in the presence of 1 M thiazole at pH 7.1, suggesting that A and A_1 are the same species with a His/Lys ligation. In fact, at neutral pH and the thiazole concentration is below 100 mM, there are four species (native form, ligand–cyt *c* complex, A_1 and A_2) co-exist in the solution (see below). Furthermore, the effect of thiazole is reversible and dialysis of the newly prepared samples with thiazole restore the spectrum of native cyt *c* (data not shown). Thus, it is concluded that the alkaline cyt *c*, A_1 and A_2 can appear at neutral pH under the presence of exogenous thiazole and concentrated thiazole stabilizes one form of them to give rise to species A.

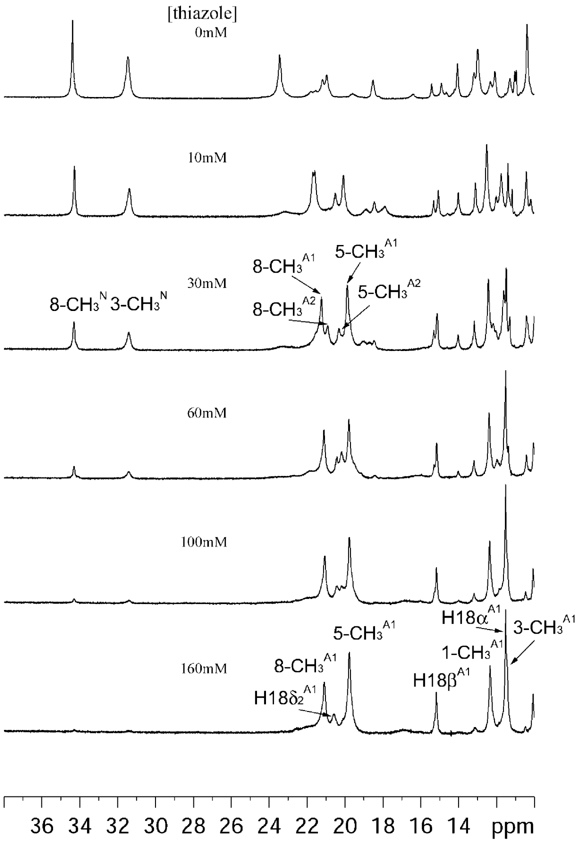

Fig. 3. The downfield hyperfine shifted region of cyt *c* spectra as a function of thiazole concentration at 303 K and pH 9.5. Resonances due to native cyt *c* and the two alkaline forms of cyt *c* are labeled with N, A_1 and A_2, respectively.

3.2. Kinetic analysis of the interconvertable process of the native form, the bound form and the alkaline forms of cyt c in the presence of thiazole

Two-dimensional EXSY is popular for its power to deal with complex multisites exchange system

Table 1
Chemical shifts of the heme methyls protons of cyt *c* in various conformations

Conformations	1-CH_3	3-CH_3	5-CH_3	8-CH_3
Native cyt *c*[a]	7.2	31.7	10.2	34.5
50 mM PBS, pH 7.0, 298 K				
CN-cyt *c*[b]	16.6	11.4	23.1	21.5
50 mM KCN, pH 7.0, 303 K				
Alkaline cyt *c*[a]	13.2	12.9	22.1	23.4
50 mM PBS, pH 10.5, 298 K				
Species A	12.2	11.5	19.8	21.3
1 M thiazole, pH 7.0, 303 K				

[a] Ref. [18].
[b] Ref. [37].

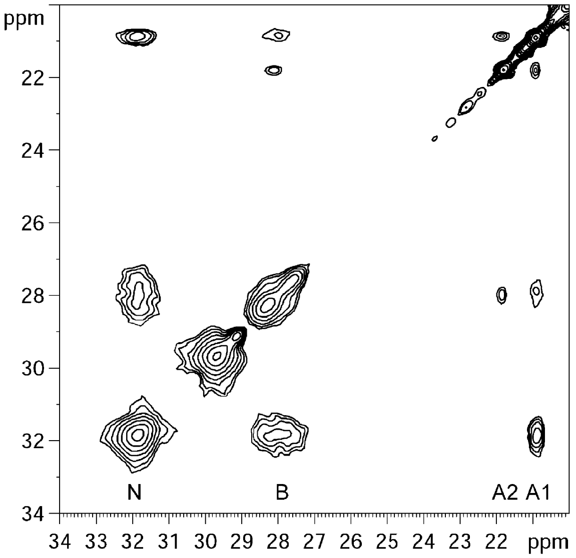

Fig. 4. Porions of the downfield region of the EXSY spectrum of cyt *c* at 323 K and pH 6.5 in the presence of 80 mM thiazole. Resonances due to native cyt *c*, thiazole-cyt *c* and the two alkaline forms of cyt *c* are labeled with N, B, A_1 and A_2, respectively.

[33]. To further understand the kinetic behaviors of the two Lys ligated forms and the thiazole–cyt *c* complex in their formation process, two-dimensional EXSY experiments are employed to evaluate the exchange rate constants between the four species (cyt *c*, thiazole–cyt *c* complex, A_1 and A_2). Fig. 4 presents the downfield region of the spectrum of cyt *c* (pH 6.5) with 80 mM thiazole at 50 °C. It can be noted that every two of the four species are exchanged to give cross-peak in the spectrum except that the exchange rate between native cyt *c* and A_2 is too slow to be detected in the EXSY spectrum at 50 °C. According to the theory of exchange spectroscopy [33], the reaction amplitude matrix **A** based on the intergration of 8-CH3 is obtained and the kinetic matrix **R** is calculated in Appendix B.

Some equilibria in the system can be presented as follows:

$$\text{cyt } c \underset{k_{21}}{\overset{k_{12}}{\rightleftharpoons}} A_1 \text{ (major form, His/Lys)} + H^+$$

$$\text{cyt } c \underset{k_{31}}{\overset{k_{13}}{\rightleftharpoons}} A_2 \text{ (minor form, His/Lys)} + H^+ \qquad (1)$$

$$\text{cyt } c + \text{thiazole} \underset{k_{41}}{\overset{k_{14}}{\rightleftharpoons}} \text{thiazole} - \text{cyt } c$$

and the exchange rate constants and the equilibrium constants can be calculated directly from matrix **R** and are listed in Table 2.

It is clear from Table 2 that in the presence of 80 mM thiazole at pH 6.5, the forward rate constants of k_{12} and k_{13} do not change noticeably compared to those of the native protein at alkaline pH in the absence of exogenous ligand, however, the reverse rate constants of k_{21} and k_{31} are significantly decreased by the exogenous thiazole by approximately 1400 folds, respectively. Thus, the pK_as of the alkaline transition of cyt *c* are decreased from approximately 9.5 to 6.1 (for A_1) and 7.6 (for A_2).

3.3. Structural characterization of species A

NMR spectroscopy was utilized to qualitatively characterize species A. The chemical shifts of heme peripheral protons were assigned by use of a combination of data from HMQC and NOESY experiments. For example, the assignments of 8-

Table 2
The exchange rate constants and the apparent equilibrium constants in cyt *c* and cyt *c* in the presence of thiazole (the errors of these parameters are approx. 10%)

	Cyt *c*, pH 9.3, 50 °C[a]	Cyt *c*, pH 9.5, 50 °C (80 mM thiazole)
k_{12} (s^{-1})	0.62	1.45
k_{21} (dm^3 mol s^{-1})	1.8×10^{9}	1.92×10^{6}
K_1 (mol/dm^3)	3.4×10^{-10}	7.55×10^{-7}
k_{13} (s^{-1})	0.14	4.41×10^{-2}
K_{31} (dm^3 mol s^{-1})	5.9×10^{8}	1.60×10^{6}
K_2 (mol/dm^3)	2.4×10^{-10}	2.75×10^{-8}
K_{14} (dm^3 mol s^{-1})	–	62.5
K_{41} (s^{-1})	–	12.3
K_3 (dm^3 mol^{-1})	–	5.08

[a] Ref. [24].

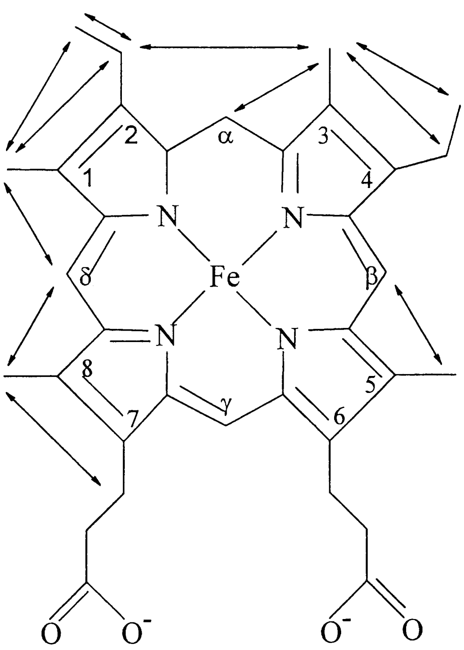

Fig. 5. Schematic representation of the dipolar connetivities observed between the heme resonances in species A.

CH_3 and 1-CH_3 were confirmed by observation of cross-peaks in the NOESY spectrum with the δ-meso proton at −4.85 ppm. The thioether CH and CH_3 resonances identified in the HMQC spectra were further confirmed by NOESY cross-peaks: NOE connectivities were observed from 1-CH_3 to CH and CH_3 of thiother-2; and from 3-CH_3 to CH and CH_3 of thiother-4. The assignments of propionate-7 and meso CHs were achieved in a similar way. In brief, Fig. 5 shows a schematic representation of the dipolar connectivities observed between the heme protons in species A, and four heme methyl resonances were clearly identified in the HMQC spectrum (Fig. 2a). The positions of the αCH and βCH2 protons of His18 were confirmed by their characteristic pattern in the TOCSY and HMQC spectra. The Hε1 and Hδ2 of His18 were identified in the one-dimensional superWEFT and superWEFT-NOE spectra. Most of the paramagnetical resonances of the heme protons and carbons have been assigned and the results are listed in Table 3. The assignments of the chemical shifts of the amino residues were achieved by first identifying the spin systems in COSY-type spectra and then correlating them in the NOESY spectra. In total, protons of approximately 30 residues have been assigned. These residues belong to the two termini, 60s-helix and regions nearby the heme. The assignments are listed in Appendix A.

NOE experiments can provide data on internuclear distances which are directly correlated with the molecular conformation. Fig. 2b represents a portion of NOEs observed between the four heme methyls and the surrounding amino residues: 8-CH_3 shows NOEs with Leu64$\delta_1 CH_3$, Leu35$\delta_1 CH_3$ and Leu35$\delta_2 CH_3$, 5-CH_3 shows NOEs with Thr28γCH_3, 1-CH_3 shows NOEs with Leu68$\delta_1 CH_3$, Leu68$\delta_2 CH_3$, Leu94$\delta_1 CH_3$ and Leu94$\delta_2 CH_3$. Inspection of the cyt *c* solution structure reveals that the distances between heme methyls and those protons mentioned above are within NOE distance (<5 Å) [34], indicating that the exchange of the axial ligand Met80 for a Lys does not alter the residues conformation around

Table 3
Assignments of the hyperfine shifted signals of the species A in the presence of 1 M thiazole at pH 7.1 and 303 K

Assignments	Chemical shifts	
	^{1}H shift (ppm)	^{13}C shift (ppm)
1-CH_3	12.17	−37.68
3-CH_3	11.46	−24.32
5-CH_3	19.80	−46.63
8-CH_3	21.33	−54.81
α-Meso	3.29	27.10
β-Meso	−2.99	13.02
δ-Meso	−4.85	37.26
Pro-7αCH_2	4.02 2.72	−9.12
Pro-7βCH_2	0.00 −0.55	72.64
2-CH	−0.82	4.66
2-CH_3	−1.27	38.47
4-CH	−1.59	−24.33
4-CH_3	−0.16	67.99
H18αCH	11.49	77.59
H18βCH_2	15.18 10.06	26.12
H18δ_2	20.29	n.d.
H18ε_1	−7.74	n.d.

the prosthetic heme significantly. At the same time, NOEs are observed clearly showing long-range interactions between N-terminal helix and C-terminal helix. For example, the α protons of Gly6 show NOEs with the α and γ protons of Leu94. A characteristic NOE pattern of $\alpha\beta(i, i+3)$ cross-peaks was also detected for residues 61–68 indicating a helix for this region (Appendix C). These results indicate that although the axial ligand Met80 is replaced by a Lys, the overall fold in cyt *c* is maintained in species A compared to the native protein. Structural modeling of alkaline *iso*-1 cyt *c* by molecular dynamics has also suggested that exchange of Met80 for a Lys does not alter the overall fold of the protein and the structure changes are almost restricted to residues 70–85 [9]. This small structural deviation from the native protein could be mainly ascribed to the property of the flexible loop encompassing residues 70–85 [35].

3.4. Effects of exogenous nitrogenous ligands on the alkaline transformation of cyt c

It has been found that imidazole, pyridine and its methyl derivatives are able to selectively stabilize one conformer of the alkaline cyt *c* at alkaline pH, and that while pyridine and its derivatives can promote the alkaline transition by decreasing the pK_a (Table 4), imidazole has little effect [23–25,36]. However, the pursuing of obtaining a ‘pure’ alkaline form of cyt *c* is still unavailable. In this paper, for the first time we find that thiazole can decrease the pK_a of the alkaline transition to as low as 6.1 and a homogenous conformer of alkaline cyt *c* is obtained at neutral pH. The mechanism of why exogenous nitrogenous ligands could promote the formation of alkaline cyt *c* is still open to debate. Our previous studies have found that 2,6-dimethyl pyridine, although hardly bind to cyt *c* due to stereo hindrance, still can facilitate the alkaline transformation [25]. This observation leads to the proposal that this promotion effect may not be related to the binding of these exogenous ligands to the heme and that these ligands just penetrate into the heme pocket, disrupt the H-bond network of the distal pocket, cause structural rearrangement and facilitate the alkaline transformation. Inspection of the solution structure of horse heart cyt *c* shows that H-bonds are observed between Thr78 HN and Pro76 O, Phe82 HN and Met80 O and Met80 S and Tyr67 OH in the distal pocket [34]. These hydrogen bonds are responsible for the stabilization of the native state and are very likely to be broken as a result of the interactions between the exogenous ligands and the heme. Work by Mauk and Nall have demonstrated that mutation at position 76 and 82 will decrease the pK_a of the alkaline transformation (Table 4). A possible explanation is that such mutations will disrupt the above mentioned H-bonds. The reason that why thiazole has the most significant effect on the alkaline transformation remains quite speculative. We propose that it may be related to the acidity. The pK_as of the conjunctive acids of thiazole, pyridine and imidazole are 2.5, 5.3 and 7.0, respectively. This sequence coincides well with the facts that thiazole is the most effective in promoting the alkaline transformation by decreasing the pK_a of this transition to as low as 6.1, while imidazole has little promotion effect on the alkaline transi-

Table 4
Effects of mutation and exogenous nitrogenous ligands on the pK_a of the alkaline transition of cyt *c*

	pK_a	Method
hh Cyt c[a]	9.5, 9.6	EXSY (pH 9.3)
iso-1 cyt *c*[b]	8.3	pH titration
iso-2 cyt *c*[c]	8.4	pH titration
Pyridine + hh cyt c[a]	7.4, 7.9	EXSY (pH 7.5 80mM pyridine)
Thiazole + hh cyt c	6.1, 7.6	EXSY (pH 6.8 80mM thiazole)
iso-1 cyt *c* mutant[b] (F82L, F82I)	~8	pH titration
iso-2 cyt c mutant[c] (P76G)	6.7	pH titration

[a] Ref. [24] values for two conformers are presented separately.

[b] Ref. [5] averaged values of the conformers.

[c] Ref. [6] averaged values of the conformers.

tion, and that the promotion ability of pyridine is the middle.

Appendix A: Chemical shifts of some residues in species A at 303 K, pH 7.1.

1	3.822	HA1	1	45	1.920	HB3	59
2	3.615	HA2	1	46	6.677	HE3	59
3	4.575	HA	2	47	6.106	HZ3	59
4	2.785	HB2	2	48	6.477	HZ2	59
5	2.680	HB3	2	49	5.731	HH2	59
6	3.444	HA	3	50	3.508	HA	61
7	2.087	HB	3	51	1.956	HB2	61
8	1.008	QG1	3	52	3.887	HA	64
9	0.977	QG2	3	53	1.092	HB2	64
10	3.854	HA1	6	54	0.953	HB3	64
11	3.196	HA2	6	55	0.735	HG	64
12	3.751	HA	11	56	−0.784	QD1	64
13	2.164	HB	11	57	−0.884	QD2	64
14	1.182	QG1	11	58	3.554	HA	65
15	1.005	QG2	11	59	2.282	HB2	65
16	6.074	HA	15	60	2.083	HB3	65
17	2.136	QB	15	61	4.794	HA	67
18	6.656	HA	19	62	3.543	HB2	67
19	5.900	HB	19	63	2.995	HB3	67
20	2.684	QG2	19	64	7.044	QD	67
21	5.195	HA	20	65	5.729	QE	67
22	2.298	HB	20	66	4.057	HA	68
23	1.151	QG1	20	67	1.626	HB2	68
24	1.044	QG2	20	68	0.729	HB3	68
25	3.454	HA	28	69	1.320	HG	68
26	3.106	HB	28	70	−0.052	QD1	68
27	−0.481	QG2	28	71	−1.099	QD2	68
28	7.000	HA	31	72	3.662	HA	94
29	3.561	HB2	31	73	1.215	QB	94
30	3.161	HB3	31	74	0.729	HG	94
31	3.188	HA	35	75	0.293	QD1	94
32	1.544	HB2	35	76	−0.173	QD2	94
33	0.104	HG	35	77	3.786	HA	96
34	−0.779	QD1	35	78	1.225	QB	96
35	−1.008	QD2	35	79	2.933	HA	98
36	4.179	HA	36	80	1.421	HB2	98
37	2.961	HB2	36	81	1.248	HG	98
38	2.647	HB3	36	82	−0.084	QD1	98
39	6.963	QD	36	83	−0.820	QD2	98
40	6.298	QE	36	84	3.924	HA	101
41	5.770	HA	54	85	0.611	QB	101
42	3.200	HB2	54	86	4.959	HA	103
43	3.060	HB3	54	87	2.849	HB2	103
44	3.033	HB2	59	88	2.494	HB3	103

Appendix B: The reaction amplitude matrix A and the kinetic matrix R

$$\mathbf{A}=\begin{bmatrix} 0.752 & 0.494 & 0 & 0.0290 \\ 0.201 & 0.810 & 0.161 & 0.0115 \\ 0 & 0.0343 & 2.41 & 0.00723 \\ 0.0685 & 0.0634 & 0.188 & 0.783 \end{bmatrix}$$

$$\mathbf{R}=\begin{bmatrix} 8.19 & -12.3 & 0.505 & -0.606 \\ -5.00 & 6.76 & -2.39 & -0.127 \\ 0.0441 & -0.507 & -17.5 & -0.100 \\ -1.45 & -0.652 & -2.60 & 4.96 \end{bmatrix}$$

Appendix C:

Fig. 6.

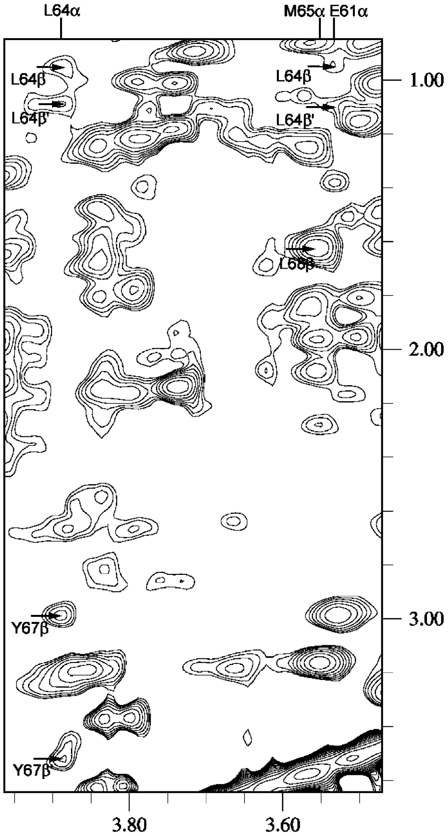

Fig. 6. Portion of NOESY indicating α-helix for residues 61-68. The cross-peaks of $\alpha\beta(i\ i+3)$ are labeled in the spectrum.

References

[1] R.E. Dickerson, R. Timkovich, in: P. Boyer (Eds.) The Enzyme, 3rd Academic Press, New York, 11, 1975, 397–547.

[2] R.A. Scott, A.G. Mauk (Eds.), Cytochrome *c*, A Multidisciplinary Approach, University Science Books, Sausalito, 1996.

[3] (a) H. Theorell, A. Akesson, Studies on cytochrome *c*. I. Electrophoretic purification of cytochrome *c* and its amino acid composition, J. Am. Chem. Soc. 63 (1941) 1804–1811
(b) H. Theorell, A. Akesson, Studies on cytochrome *c*. II. The optical properties of pure cytochrome c and some of its derivatives, J. Am. Chem. Soc. 63 (1941) 1812–1818
(c) H. Theorell, A. Akesson, Studies on cytochrome *c*. III. Titration curves, J. Am. Chem. Soc. 63 (1941) 1818–1820.

[4] X.L. Hong, D.W. Dixon, NMR study of the alkaline isomerization of ferricytochrome *c*, FEBS Lett. 246 (1989) 105–108.

[5] L.L. Pearce, A.L. Gartner, M. Smith, A.G. Mauk, Mutation-induced perturbation of the cytochrome *c* alkaline transition, Biochemistry 28 (1989) 3152–3156.

[6] B.T. Nall, E.H. Zuniga, T.B. White, L.C. Wood, L. Ramdas, Replacement of a conserved proline and the alkaline conformational change in *iso*-2-cytochrome *c*, Biochemistry 28 (1989) 9834–9839.

[7] W.B. Pollock, F.I. Rosell, M.B. Twitchett, M.E. Dumont, A.G. Mauk, Bacterial expression of a mitochondrial cytochrome c. Trimethylation of lys72 in yeast *iso*-1-cytochrome *c* and the alkaline conformational transition, Biochemistry 37 (1998) 6124–6131.

[8] F.I. Rosell, J.C. Ferrer, A.G. Mauk, Proton-linked protein conformational switching: definition of the alkaline conformational transition of yeast *iso*-1-ferricytochrome *c*, J. Am. Chem. Soc. 120 (1998) 11234–11245.

[9] S.R. Ness, T.P. Lo, A.G. Mauk, Structural models for the alkaline conformers of yeast *iso*-1-ferricytochrome *c*, Isreal J. Chem. 40 (2000) 21–25.

[10] F.I. Rosell, T.R. Harris, D.P. Hildebrand, S. Dopner, P. Hildebrandt, A.G. Mauk, Characterization of an alkaline transition intermediate stabilized in the Phe82Trp variant of yeast *iso*-1-cytochrome *c*, Biochemistry. 39 (2000) 9047–9054.

[11] C. Weber, B. Michel, H.R. Bosshard, Spectroscopic analysis of the cytochrome *c* oxidase–cytochrome *c* complex: circular dichroism and magnetic circular dichroism measurements reveal change of cytochrome *c* heme geometry imposed by complex formation, Proc. Natl. Acad. Sci. USA 4 (1987) 6687–6691.

[12] S. Dopner, P. Hildebrandt, F.I. Rosell, A.G. Mauk, M. von Walter, G. Buse, et al., The structural and functional role of lysine residues in the binding domain of cytochrome *c* in the electron transfer to cytochrome *c* oxidase, Eur. J. Biochem. 261 (1999) 379–391.

[13] G.A. Elove, A.K. Bhuyan, H. Roder, Kinetic mechanism of cytochrome *c* folding: involvement of the heme and its ligands, Biochemistry 33 (1994) 6925–6935.

[14] W. Colon, L.P. Wakem, F. Sherman, H. Roder, Identification of the predominant non-native histidine ligand in unfolded cytochrome *c*, Biochemistry 36 (1997) 12535–12541.

[15] S.R. Yeh, S. Takahashi, B. Fan, D.L. Rousseau, Ligand exchange during cytochrome *c* folding, Nat. Struct. Biol. 4 (1997) 51–56.

[16] S.R. Yeh, D.L. Rousseau, Folding intermediates in cytochrome *c*, Nat. Struct. Biol. 5 (1998) 222–228.

[17] S.R. Yeh, D.L. Rousseau, Ligand exchange during unfolding of cytochrome *c*, J. Biol. Chem. 274 (1999) 17853–17859.

[18] B.S. Russell, R. Melenkivitz, K.L. Bren, NMR investigation of ferricytochrome *c* unfolding: detection of an equilibrium unfolding intermediate and residual structure in the denatured state, Proc. Natl. Acad. Sci. USA 97 (2000) 8312–8317.

[19] B.S. Russell, K.L. Bren, Denaturant dependence of equilibrium unfolding intermediates and denatured state structure of horse ferricytochrome *c*, J Biol Inorg Chem. 7 (2002) 909–916.

[20] B. Hammack, S. Godbole, B.E. Bowler, Cytochrome c folding traps are not due solely to histidine-heme ligation: direct demonstration of a role for N-terminal amino group-heme ligation, J. Mol. Biol. 275 (1998) 719–724.

[21] C.J. Nelson, B.E. Bowler, pH dependence of formation of a partially unfolded state of a Lys73 → His variant of *iso*-1-cytochrome *c*: implications for the alkaline conformational transition of cytochrome c, Biochemistry 39 (2000) 13584–13594.

[22] S. Sivakoludu, P.A. Mabrouk, Insights into the alkaline transformation of ferricytochrome *c* from ^{1}H NMR studies in 30% acetonitrile–water, Protein Sci. 10 (2001) 2291–2300.

[23] W. Shao, Y. Yao, G. Liu, W. Tang, ^{1}H NMR studies of pyridine binding to cytochrome *c*, Inorg. Chem. 32 (1993) 6112–6114.

[24] J. Lu, G. Liu, Y. Chen, W. Tang, D. Zhu, Effects of pyridine on the alkaline isomerization of cytochrome *c*, Inorg. Chim Acta. 275–276 (1998) 58–64.

[25] J. Lu, D. Ma, J. Hu, W. Tang, D. Zhu, NMR studies of the effects of nitrogenous ligands on the alkaline isomerization of cytochrome *c*, Spectrosc. Lett. 32 (1999) 519–533.

[26] D.L. Brautigan, S.F. Miller, E. Margoliash, Mitochondria cytochrome *c*: preparation and activity of native and chemically modified cytochrome *c*, Methods Enzymol. 53D (1978) 128–164.

[27] T. Inubushi, E.D. Becker, Efficient detection of paramagnetically shifted NMR resonances by optimizing the WEFT pulse sequence, J. Magn. Reson. 51 (1983) 128–133.

[28] L. Banci, I. Bertini, C. Luchinat, M. Piccioli, A. Scozzafava, P. Turano, ^{1}H NOE studies on dicopper (II)

dicobalt (II) superoxide dismutase, Inorg. Chem. 28 (1989) 4650–4656.

[29] K. Wuthrich, NMR of Proteins and Nucleic Acids, Wiley, New York, 1986.

[30] R. Timkovich, Heteronuclear multiple quantum coherence NMR spectroscopy of paramagnetic heme and cytochrome c_{551}, Inorg. Chem. 30 (1991) 37–42.

[31] C. Bartels, T. Xia, M. Billeter, P. Guntert, K. Wuthrich, The program XEASY for computer-supported NMR spectral analysis of biological macromolecules, J. Biomol. NMR 5 (1995) 1–10.

[32] G.R. Moore, G.W. Pettigrew, Cytochrome *c*, Evolutionary Structural and Physiological Aspects, Springer-Verlag, Berlin, 1990.

[33] R.R. Ernst, G. Bodenhausen, A. Wokaun, Principles of Nuclear Magnetic Resonances in One and Two Dimensions, Oxford University Press, Oxford, 1987.

[34] L. Banci, I. Bertini, H.B. Gray, C. Luchinat, T. Reddig, A. Rosato, et al., Solution structure of oxidized horse heart cytochrome *c*, Biochemistry 36 (1997) 9867–9877.

[35] Y. Bai, T.R. Sosnick, L. Mayne, S.W. Englander, Protein folding intermediates: native-state hydrogen exchange, Science 269 (1995) 192–197.

[36] L. Banci, I. Bertini, G. Liu, J. Lu, T. Reddig, W. Tang, et al., Effects of extrinsic imidazole ligation on the molecular and electronic structure of cytochrome *c*, J. Biol. Inorg. Chem. 6 (2001) 628–637.

[37] Y. Yao, C. Qian, K. Ye, J. Wang, Z. Bai, W. Tang, Solution structure of cyanoferricytochrome *c*: ligand-controlled conformational flexibility and electronic structure of the heme moiety, J. Biol. Inorg. Chem. 7 (2002) 539–547.